

Mars, P., and D. W. van Krevelen, "Oxidation-Reduction Catalytic Reactions," *Chem. Eng. Sci. Special Suppl.*, 3, 41 (1949).
 Smith, J. M., *Chemical Engineering Kinetics*, 3rd Ed., 343, McGraw-Hill, New York (1981).
 Sreeramamurthy, R., and P. G. Menon, "Oxidation of H_2S on Active Carbon Catalyst," *J of Cat.*, 37, 287 (1975).
 Steijns, M., F. Derks, A. Verloop, and P. Mars, "The Mechanism of the

Catalytic Oxidation of Hydrogen Sulfide. II: Kinetics and Mechanism of Hydrogen Sulfide Oxidation Catalyzed by Sulfur," *J. of Cat.*, 42, 87 (1976).

Manuscript received April 19, 1983; revision received June 3, and accepted June 23, 1983.

Mechanistic Models for Transitions between Regimes of Fluidization

WEN-CHING YANG

Research and Development Center
 Westinghouse Electric Corporation
 Pittsburgh, PA 15235

INTRODUCTION

Understanding the flow regime transitions is important because different flow regimes provide vastly different solid circulation patterns, solids and gas mixing rates, and thus the chemical reaction rates. They, in turn, dictate the reactor design considerations. There are very few theoretical discussions and correlations available in the literature on the criteria of flow transitions between these different regimes. This paper attempts to develop mechanistic models to predict these flow transitions for fine particles generally belonging to Geldart's Class A (1973).

GENERAL FLUIDIZATION REGIME DIAGRAM

A qualitative fluidization map for fine particles was initially proposed by Yerushalmi et al. (1978) and refined later in Yerushalmi and Cankurt (1979). A more recent and more general fluidization regime diagram was presented by Li and Kwauk (1980), Figure 1. The log-log coordinates are used here, instead of the original semilogarithmic presentation, to show the approximately straight-line relationship in different regimes, which will become more apparent later. Use of the voidage as the ordinate and the gas

velocity as the abscissa allows a convenient presentation for fluidization regimes from incipient fluidization all the way to dilute-phase pneumatic transport. Different fluidization regimes simply exhibit different voidage-gas velocity relations.

THEORY OF CLUSTER FORMATION

The application of the concept of cluster formation was first suggested by Yerushalmi et al. (1978). Matsen (1982) also used it in his analysis of choking and entrainment mechanisms. A quantitative theory, however, was first proposed by Capes (1974) for application to the fluidization of fine particles. He followed the development of the concept of flocs during sedimentation by Scott (1968) and modified the Richardson and Zaki equation (1954) to include an "effective" porosity, as shown in Eq. 1.

$$\frac{U}{U_t} = \epsilon_e^m = (1 - KC)^m \quad (1)$$

The "effective" porosity, ϵ_e , includes the void space between aggregates (or clusters) only while ϵ , the apparent voidage, includes also the void space between solid particles inside the clusters. He attributed the large values of n in the Richardson and Zaki equation often reported in the literature for fine particles (ranging up to a value of 10) to the increased effective particle volume caused by agglomeration or to the irregular particle shape, which immobilized a layer of fluid in the surface irregularities. Using Eq. 1 with the "effective" voidage brings the exponent m within the range of the original Richardson and Zaki equation.

The bed density reported by Yerushalmi and Cankurt (1979) and the voidage-gas velocity relation reported by Li and Kwauk (1980) were processed to give the best fit using the original Richardson and Zaki equation and the modified one shown in Eq. 1. The results are summarized in Table 1. The U_t can be considered to be the terminal velocity of a cluster with the "effective" particle diameter. In fitting Eq. 1 to the experimental data, the procedure Capes (1974) suggested was followed. The calculation was carried out until the value of m and n agreed to within 0.02. The successful correlation of these experimental data indicates that, hydrodynamically, these fluid beds are similar to beds with "clusters" of finite sizes.

CONTINUITY WAVE AND TRANSITION FROM BUBBLING TO TURBULENT FLUIDIZATION

The continuity wave exists as a quasisteady-state phenomenon whenever there is a relation between the steady equilibrium flow

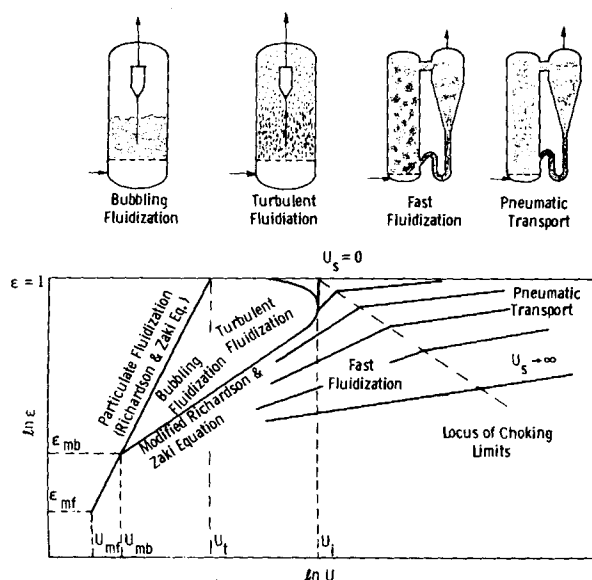


Figure 1. Schematic fluidization regime diagram (Li and Kwauk, 1980).

TABLE 1. RESULTS OF FITTING EXPERIMENTAL DATA WITH ORIGINAL AND MODIFIED RICHARDSON AND ZAKI EQUATIONS (EQS. 1 AND 2)

Data Source	Bed Material	n	Correlation Coefficient	m	K	U_t , cm/s	Correlation Coefficient
Yerushalmi & Cankurt (1979)	Dicalite 4200	16.34	0.9618	2.72	3.76	336	-0.9420
	FCC Catalyst	6.32	0.9891	2.50	1.75	398	-0.9876
	HFZ-20 Catalyst	5.15	0.9854	2.44	1.45	545	-0.9906
	No. 85 Sand	4.07	0.9584	2.39	1.39	814	-0.9703
Li & Kwauk (1980)	Fine Alumina	8.31	0.9061	3.03	1.90	232	-0.8797

rate of a substance and its concentration. The development of the basic equations was provided by Wallis (1969). The same approach is now employed here to predict the transition from bubbling to turbulent fluidization.

The drift flux between the fluid and the solids is defined as:

$$j_{fs} = -j_{sf} = (1 - \epsilon_e)j_f - \epsilon_e j_s \quad (2)$$

with the positive direction to be upward. The solids are assumed to form clusters with an "effective" porosity ϵ_e . The continuity wave velocity in a dispersion of particles was derived by Wallis (1969) as:

$$V_w = j + \frac{\partial}{\partial \epsilon_e} (j_{fs}); j = j_f + j_s \quad (3)$$

In the bubbling and turbulent fluidization regimes no net transport of solids occurs and thus:

$$j_s = \frac{W_s}{\rho_s A} = 0 \text{ and } j_f = \frac{Q_f}{A} = U. \quad (4)$$

The continuity wave velocity (Eq. 3) becomes

$$V_w = U + \frac{\partial}{\partial \epsilon_e} [(1 - \epsilon_e)U]. \quad (5)$$

Combining Eqs. 1 and 5, we have the continuity wave velocity for the bubbling and turbulent fluidization regimes as

$$V_w = U_i m (1 - \epsilon_e) \epsilon_e^{m-1}. \quad (6)$$

Yerushalmi and Cankurt (1979) observed experimentally that the transition from bubbling fluidization to turbulent fluidization is reflected in the fluctuations of both the local dynamic pressure and the total pressure drop across the bed. The bubbling-to-turbulent-fluidization transition with maximum pressure fluctuation was assumed to occur at a voidage corresponding to the maximum continuity wave velocity in this analysis. Differentiating Eq. 6 and setting it to zero, we have, at the bubbling-to-turbulent-fluidization transition,

$$\epsilon_e = \frac{m-1}{m} \text{ or } \epsilon = 1 - \frac{1-\epsilon_e}{K} \quad (7)$$

At an "effective" porosity, ϵ_e , less than $(m-1)/m$, the continuity wave velocity, V_w , increases with increases in ϵ_e . When ϵ_e is larger than $(m-1)/m$, V_w decreases with increases in ϵ_e . Substituting the values of m , K and U_i in Table 1 into Eqs. 1 and 7, we can calculate the gas velocity and voidage at transition and compare them with those observed experimentally in Table 2. With our current understanding of this phenomenon, the reasonable agreement shown in Table 2 is encouraging. The average diameter

of the clusters at transition, the number of individual particles making up each cluster, and the density of each cluster, are also calculated and reported in Table 2.

TRANSPORT VELOCITY

When the operating gas velocity is higher than a so-called transport velocity, a sharp increase in carry-over occurs, and the bed becomes essentially an entrained bed. New feed or recycling of solids is required to maintain operation of the bed. Depending on the operating gas velocity and the solid loading, the transport reactor can be either in dilute-phase or in dense-phase pneumatic transport, also called fast fluidized bed, as shown in Figure 1. In this analysis we have assumed the transport velocity of each system to be equal to the terminal velocity of the cluster, U_t . The results are compared with those observed experimentally in Table 2.

DILUTE-PHASE PNEUMATIC TRANSPORT AND FAST FLUIDIZATION

Yerushalmi and Cankurt (1979) observed pistonlike movement of solids for the larger solids they used in their experiments, a phenomenon similar to the slugging transition between dilute- and dense-phase pneumatic transport and predictable from existing choking correlations (Yang, 1976). For fine particles, Yousfi and Gau (1974) observed experimentally that the transition between dilute- and dense-phase transport did not produce solids slugs extending across the cross section of the pipe, but rather solids "bundles." It is also clear from the fluidization regime map experimentally produced by Li and Kwauk (1980) and shown in Figure 1 that the dilute-phase pneumatic transport and the fast fluidization (dense-phase transport bed) have similar characteristics in the voidage-gas velocity plot. The difference in dependence of the voidage and the gas velocity is due to the difference in the gas-solids slip velocity created by cluster formation. It is logical, then, to expect that the transition between the dilute-phase pneumatic transport and the fast fluidization regimes can be approximated by the choking correlations developed for pneumatic transport.

Yang (1982) recently proposed an empirical correlation for choking using data from Yousfi and Gau (1974), who experimentally determined the gas velocity and the voidage at choking. The correlation is presented in Eq. 8.

$$\frac{U}{U_t} = \epsilon^q; q = -33.2 + 1.18 (Re)_t \text{ for } (Re)_t < 23 \quad (8)$$

TABLE 2. COMPARISON OF CALCULATED AND EXPERIMENTAL PARAMETERS AT BUBBLING-TURBULENT FLUIDIZATION TRANSITION

Data Source	Bed Material	Transition Velocity, cm/s		Transition Voidage		Cluster Size, μm	Number of Particles in a Cluster	Density of the Cluster, g/cm ³	Transport Velocity, cm/s	
		Exp.	Calc.	Exp.	Calc.				Exp.	Calc.
Yerushalmi & Cankurt (1979)	Dicalite 4200	53-107	97	0.877-0.910	0.902	595	1.6×10^3	0.44	—	336
	FCC Catalyst	61	108	0.692	0.771	1,461	1.5×10^4	0.61	120-150	398
	HFZ-20 Catalyst	91-137	151	0.640-0.716	0.718	1,138	8.6×10^3	1.00	~210	545
	No. 85 Sand	274-550	223	0.750-0.860	0.699	1,223	68	1.91	—	814
Li & Kwauk (1980)	Fine Alumina	~100	69	~0.85	0.826	272	67	1.66	~230	232

TABLE 3. COMPARISON OF EXPERIMENTAL AND CALCULATED TRANSITION POINT BETWEEN DILUTE-PHASE PNEUMATIC TRANSPORT AND FAST FLUIDIZATION (DENSE-PHASE TRANSPORT)

Superficial Particle Velocity, cm/s	Material—Fine Alumina (Li and Kwauk, 1980) Gas Velocity at Transition, cm/s	Voidage at Transition	
		Experimental	Calculated
0.076	250	0.985	0.949
0.491	310	0.975	0.942
1.81	415	0.945–0.970	0.933
2.57	450	0.935–0.950	0.931
4.05	475	0.930	0.929

The results from Eq. 8 compared favorably with the experimental data obtained by Li and Kwauk (1980) on the transition between dilute-phase pneumatic transport and fast fluidization, Table 3.

EMPIRICAL CORRELATIONS FOR TRANSITION OF FLUIDIZATION

The mechanistic model proposed for transition between the bubbling and turbulent fluidization cannot be applied a priori because the dependence of the cluster size on operating conditions and particle characteristics is unknown. We found, however, that for the three finer particles used by Yerushalmi and Cankurt (Solids A, B and C), the transition points between bubbling and turbulent fluidization can be correlated with high accuracy by the following equations:

$$K = 0.883 (Re)_t^{-0.485} \text{ correlation coefficient} = -0.9994 \quad (9)$$

$$m = 2.31 (Re)_t^{-0.0547} \text{ correlation coefficient} = -0.9979 \quad (10)$$

$$\frac{U_t}{U_i} = 25.49 (Re)_t^{-0.582} \text{ correlation coefficient} = -0.9880 \quad (11)$$

In the absence of other correlations, Eqs. 9 to 11 can be used for quantitative criteria to predict the transition between bubbling and turbulent fluidization for fine particles.

NOTATIONS

A	= cross-sectional area of a fluidized bed or a pipe
C	= volumetric fraction of solids, $C = 1 - \epsilon$
d_p	= particle diameter
j	= mixture volumetric flux, $= j_f + j_s$
j_f, j_s	= volumetric fluxes of fluid and solids respectively
j_{fs}, j_{sf}	= drift fluxes defined in Eq. 2
K	= volume of aggregates (clusters) per unit volume of solid
m	= exponent in the modified Richardson and Zaki equation (Eq. 1)

n	= exponent in the Richardson and Zaki equation
q	= exponent in Eq. 8
Q_f	= volumetric flow rate of the fluid
$(Re)_t$	= Reynolds number $= d_p U_t \rho_f / \mu$
U	= superficial fluid velocity
U_t	= terminal velocity of a cluster
U_i	= terminal velocity of a single particle
V_w	= continuity wave velocity defined in Eq. 3
W_s	= solid flow rate
ϵ	= voidage
ϵ_e	= "effective" voidage defined in Eq. 1, $\epsilon_e = 1 - KC$
μ	= fluid viscosity
ρ_f	= density of the fluid
ρ_s	= density of the solids

LITERATURE CITED

- Capes, C. E., "Particle Agglomeration and the Value of the Exponent n in the Richardson-Zaki Equation," *Powder Tech.*, **10**, 303 (1974).
 Geldart, D., "Type of Gas Fluidization," *Powder Tech.*, **7**, 285 (1973).
 Li, Y., and M. Kwauk, "The Dynamics of Fast Fluidization," *Fluidization*, Grace and Matsen, Eds., Plenum Press, New York (1980).
 Richardson, J. F., and W. N. Zaki, "Sedimentation and Fluidization: Part I," *Trans. Inst. Chem. Eng.*, **32**, 35 (1954).
 Scott, K. J., "The Thickening of Calcium Carbonate Slurries," *Ind. Eng. Chem. Fund.*, **1**, 484 (1968).
 Wallis, G. B., *One-Dimensional Two-Phase Flow*, McGraw-Hill, New York (1969).
 Yang, W. C., "A Criterion for Fast Fluidization," *Proc. of Third Int. Conf. on Pneumatic Transport of Solids in Pipes*, E5 (1976).
 Yang, W. C., "Criteria for Choking in Vertical Pneumatic Conveying Lines," *Powder Tech.*, **35**, 143 (1983).
 Yerushalmi, J., N. T. Cankurt, D. Geldart, and B. Liss, "Flow Regimes in Vertical Gas-Solid Contact Systems," *AIChE Symp. Ser.*, **74**, No. 176, 1 (1978).
 Yerushalmi, J., and N. T. Cankurt, "Further Studies of the Regimes of Fluidization," *Powder Tech.*, **24**, 187 (1979).
 Yousfi, Y., and G. Gau, "Aerodynamics of the Vertical Flow of Concentrated Gas-Solids Suspensions-I. Flow Regimes and Aerodynamic Stability," *Chem. Eng. Sci.*, **29**, 1939 (1974).

Manuscript received April 19, 1983; revision received July 7, and accepted July 14, 1983.